THE ASTROPHYSICAL JOURNAL, 491:501–507, 1997 December 20

THE EMISSIVE MECHANISM OF FLAT-SPECTRUM RADIO SOURCES

JIANCHENG WANG, XUEFENG CEN, JUN XU, AND TONGLING QIAN
Yunnan Observatory, Chinese Academy of Sciences, P.O. Box 110, Kunming, Yunnan Province, People's Republic of China
Received 1997 March 27; accepted 1997 August 4

ABSTRACT

An optically thin synchrotron emission model based on evolutionary relativistic electron spectra is developed to explain radio flat spectra of blazars. The basic physical processes of relativistic electron spectrum evolution for synchrotron emission are second-order Fermi acceleration of turbulent plasma waves, Fermi acceleration of shock waves, radiation loss, particle escape, and adiabatic deceleration in a flow of synchrotron plasma. When the timescale of turbulence acceleration is larger than the Alfvén timescale, the evolutionary spectra of relativistic electrons are flattened in low energy and steepen rapidly in high energy. The shape of relativistic electron spectra depends on the level of plasma turbulence and shock wave acceleration. In the case of strong plasma turbulence, the resulting synchrotron emission has a flatter spectrum below a special frequency ν_c, which is inversely proportional to magnetic field, plasma density, and the square of emission region size. In the case of weak plasma turbulence, the flat spectrum is not formed by the physical processes in the plasma. Based on this model, the radio flat-spectrum sources are easily formed in compact active galactic nuclei. The flat radio sources with higher frequency extension appear in compact, active nuclei with lower plasma density and magnetic field.

Subject headings: galaxies: active — galaxies: nuclei — MHD — radiation mechanisms: nonthermal — turbulence

1. INTRODUCTION

The flat radio spectra in some classes of active galactic nuclei (AGNs), such as blazars, have been attributed to self-absorption (Kellermann & Pauliny-Toth 1969). The specific geometric properties of the source constrain the flat spectra to extend over a larger range in radio frequency (Marscher 1977). This model is not consistent with interferometric data, in which the linear size of the source is inversely proportional to frequency (Cotton et al. 1980). The evidence for flat, optically thin spectra in some AGNs has been presented by O'Dell et al. (1988) and Hughes, Aller, & Aller (1989b; Hughes et al. 1991). Radio flat-spectrum sources are also observed in the Galactic center (GC) region that are not self-absorbed (Yusef-Zadeh 1989). It is suggested here that optically thin synchrotron emission due to a hard electron spectrum produced through the acceleration processes in turbulent plasma can explain the nature of flat-spectrum sources.

Shock wave and Fermi acceleration in turbulent plasma to produce special spectra of relativistic electrons have been presented by many authors—for example, a synchrotron pileup model of infrared/optical emission by Schlickeiser (1984) and a model of the flat-spectrum sources in the Galactic center region by Anantharamaiah et al. (1991). Hard electron spectra from acceleration alone have been discussed by many authors (Heavens & Drury 1989; Achterberg 1990; Schneider 1993; Melrose & Pope 1993). Melrose (1996) has emphasized that it is plausible for flat or weakly inverted synchrotron spectra in the GC region and in AGNs to form hard electron spectra due to Fermi acceleration or multiple diffusive shock acceleration coupled with synchrotron losses. The current view of flat-spectrum radio sources is of a slightly diverging flow of synchrotron plasma, within which a flaring of the flow, a recollimation shock, or the optically thick surface define a "base" (Marscher & Gear 1985; Hughes, Aller, & Aller 1989a, 1989b). Based on this physical scenario, we study the emissive mechanism in detail. The basic physical processes of relativistic electron spectrum evolution for synchrotron emission are second-order Fermi acceleration of turbulent plasma waves, Fermi acceleration of shock waves, radiation loss, particle escape, and adiabatic deceleration in a flow of synchrotron plasma.

2. THE EVOLUTION OF RELATIVISTIC ELECTRON SPECTRA

2.1. *Basic Equation*

We consider the behavior of relativistic electrons in a flow of turbulent plasma carrying a magnetic field and diffusive shock waves. For all interactions the momentum gain or loss for single electrons can be calculated for given astrophysical parameters (thermal gas density n_e, shock wave velocity V_s, magnetic field B, etc.; Schlickeiser 1984); an evolutionary equation in momentum space for the electron is (Schlickeiser 1984)

$$\frac{\partial f}{\partial t} = \frac{1}{p^2}\frac{\partial}{\partial p}\left[p^4\left(a_2\frac{f}{p} + \beta f\right)\right] - \frac{a_1}{p^2}\frac{\partial}{\partial p}(p^3 f) - \frac{f}{T} + Q(p, t)\,, \tag{1}$$

where $N(p, t) = 4\pi p^2 f(p, t)$ is the number of particles per unit momentum and unit volume, $Q(p, t)$ represents relativistic electron–injected sources, and T is escape time from the plasma.

$$a_1 = kV_s^2/4K_{\parallel} - a_3\,, \tag{2}$$

$$a_2 = V_{\rm A}^2/9K_{\parallel}\,, \tag{3}$$

$$\beta = \left(\frac{4}{3}\right)\left[\frac{\sigma_{\rm T} c^2}{(m_e c^2)^2}\right](W_H + W_{\rm ph})\,, \tag{4}$$

where $K_{\parallel}$ is the spatial diffusion coefficient; k is the filling factor of diffusive shock waves; W_H and $W_{\rm ph}$ are the energy densities of magnetic fields and of ambient photon fields; $V_{\rm A}$ and V_s are the Alfvén velocity and the speed of the shock

wave; a_3 (=div $V/3 + \delta n_i$) gives the energy loss ratios of adiabatic expansion with velocity V and nonthermal bremsstrahlung of the plasma (n_i is plasma density, and δ is the rate of nonthermal bremsstrahlung losses, which is a constant).

2.2. *Basic Assumption*

Throughout this work we assume that $K_{\parallel}$ is momentum independent and is defined as

$$K_{\parallel} = \tfrac{1}{9}\eta V_{\rm A} L\,, \tag{5}$$

where η is a dimensionless parameter that determines the order amount of the spatial diffusion coefficient $K_{\parallel}$, and L is the size of the plasma. The timescale of turbulent acceleration T_a is

$$T_a = \frac{1}{a_2} = \eta\left(\frac{L}{V_{\rm A}}\right), \tag{6}$$

which is proportional to η. The parameter η is important; it shows the ratio of the timescale of turbulence acceleration to the Alfvén timescale. In this work we first examine the case of $\eta > 1$ in detail; that is, the timescale of turbulence acceleration is larger than the Alfvén timescale, the maximum power input into relativistic electrons will involve an initial flux of Alfvén waves due to plasma instability driven by activities of center nuclei. The power input in turbulence is

$$\dot{W}_{\rm turb} = \left(\frac{W_{\rm turb}}{W_B}\right)\left(\frac{V_{\rm A}}{L}\right)W_B\,. \tag{7}$$

We also assume equipartition of energy between relativistic electrons and magnetic field ($W_e = W_B$); the power accelerating relativistic electrons is

$$\dot{W}_e = a_2 W_e = \left(\frac{1}{\eta}\right)\left(\frac{V_{\rm A}}{L}\right)W_B\,. \tag{8}$$

If two powers balance each other, that is,

$$\left(\frac{1}{\eta}\right)\left(\frac{V_{\rm A}}{L}\right) \simeq \left(\frac{W_{\rm turb}}{W_B}\right)\left(\frac{V_{\rm A}}{L}\right), \tag{9}$$

then $\eta \simeq W_B/W_{\rm turb}$ will be a measure of the level of the turbulence in the plasma. The parameters a_1, a_2 are constants with respect to momentum. The escape time T, which combines the effects of spatial diffusion, is given by (Lesch & Schlickeiser 1985)

$$T = \frac{2K_{\parallel}}{c^2\alpha}\,, \tag{10}$$

where $\alpha = (\pi^2/3)$, and

$$\tau_0 = \frac{cL}{2K_{\parallel}} = \frac{9}{2\eta}\left(\frac{c}{V_{\rm A}}\right), \tag{11}$$

where c is the speed of light. T is given by

$$T = \frac{27}{2\pi^2\eta}\left(\frac{L}{V_{\rm A}}\right)\left(1 + \frac{4}{27}\,\eta\bar{V}_{\rm A}\right)^2, \tag{12}$$

where $\bar{V}_{\rm A} = V_{\rm A}/c$ is the Alfvén velocity in units of the speed of light and should be less than unity. It shows that the escape time is dependent on η, $V_{\rm A}$, and L. The evolution of the electron spectrum is determined by assuming a certain background distribution of magnetic field, radiation, and matter, a_1, a_2 and β are functions of time, but it is not clear how they evolve, so we assume they evolve only slowly compared to the time for the electron distribution to evolve, and treat them as constants while solving for $N(p, t)$.

2.3. *Basic Solution*

We are interested in the steady state solution of equation (1). Using a set of parameters

$$X = p/p_c\,, \quad X_0 = p_0/p_c \tag{13}$$

and

$$a = \frac{a_1}{a_2}\,, \quad \varepsilon = \frac{1}{a_2 T}\,, \quad \mu = \left[\varepsilon + \left(\frac{a+3}{2}\right)^2\right]^{1/2} \tag{14}$$

with $p_c = a_2/\beta$, a steady state solution given by Schlickeiser (1984) is

$$N(X) \propto \int_0^{\infty} dX_0\, Q(X_0) G(X, X_0)\,, \tag{15}$$

where the Green's function of equation (1) is

$$G(X, X_0) \sim X_0^{b+2} X^{c-b+4} e^{-X} \times \begin{cases} U(b, c, X_0)M(b, c, X) & \text{for } X \le X_0\,, \\ M(b, c, X_0)U(b, c, X) & \text{for } X > X_0\,, \end{cases} \tag{16}$$

and $b = \mu - (a+3)/2$, $c = 1 + 2\mu$, where U and M are confluent hypergeometric functions (Abramowitz & Stegun 1970), and $Q(X)$ is the initial electron distribution.

2.4. *Resulting Electron Spectra*

We first consider the selection of the parameters p_c, ε, n_e, B, etc. For a synchrotron source, the radio wave cannot be absorbed by inverse bremsstrahlung. A constraint on thermal electron density and temperature of the plasma is presented:

$$n_e < 7.0 \times 10^4\left(\frac{T}{10^4\ {\rm K}}\right)^{3/4}\left(\frac{L}{0.1\ {\rm pc}}\right)\left(\frac{\nu}{\rm GHz}\right)\ {\rm cm}^{-3}\,, \tag{17}$$

where L is the size of compact radio sources. The estimated magnetic field in compact radio sources is in the range 10^{-3} G $< B < 10^2$ G (Kellermann & Pauliny-Toth 1969). In general the synchrotron radiation is the main loss process of relativistic electrons in the radio region; we ignore the Compton emissive loss. Then

$$\frac{p_c}{m_e c} = \frac{a_2}{m_e c\beta} = 5.49 \times 10^3 \eta^{-1}\left(\frac{L}{0.1\ {\rm pc}}\right)^{-1} \times \left(\frac{B}{10^{-3}\ {\rm G}}\right)^{-1}\left(\frac{n_e}{10^4\ {\rm cm}^{-3}}\right)^{-1/2}; \tag{18}$$

ε is the ratio of the second-order Fermi acceleration timescale to the electron escape timescale with

$$\varepsilon = \frac{1}{a_2 T} = 0.73\eta^2\left(1 + \frac{4}{27}\,\eta\bar{V}_{\rm A}\right)^{-2}, \tag{19}$$

which is dependent on the characteristic parameter η and the Alfvén velocity $V_{\rm A}$; a is a special parameter describing the shock wave acceleration effect. For the acceleration phase by shock waves we expect $a > 0$. For the equilibrium phase of shock wave acceleration balancing bremsstrahlung and adiabatic deceleration losses, we expect $a = 0$. For the deceleration by bremsstrahlung and heavy adiabatic expansion of the plasma, $a < 0$ is expected. In what follows we calculate the evolution of relativistic electron spectra.

Assuming the initially momentum steady state source distribution $Q(p) = Q_0 p^{-\alpha-2}$ $(p_1 \leq p \leq p_2)$,where α is the spectral index of relativistic electrons, we calculate the steady state electron density from equations (13) and (14) in the numerical methods (see Appendix). Depending on the value of a and ε, the steady state spectrum is shown in Figure 1. The steady state spectrum has several features: (1) In the case of strong turbulence or $\eta \sim 1$, it has a flat shape below p_c and appears as a weak pileup in the high-energy part when the shock wave acceleration occurs; then it steepens rapidly in the high-energy end. The flat spectrum is weakly dependent on the initial spectral index. (2) In the case of weak turbulence or $\eta \gg 1$, the initial spectrum is weakly affected by the physical processes in the plasma. The flat spectrum is not easily formed. (3) The energy range of the flat spectrum moves to high energy with increasing shock wave acceleration a. (4) The resulting spectral shape is weakly dependent on the cutoff energies of the initial spectrum.

In the case $\eta < 1$, that is, the timescale of turbulence acceleration is shorter than the Alfvén timescale, or the electron escape timescale is larger than the turbulence timescale, radiation losses combined with acceleration can lead the relativistic electron spectrum to form a pileup at the critical momentum p_c, in which the average energy gain due to acceleration balances the radiation loss. This pileup

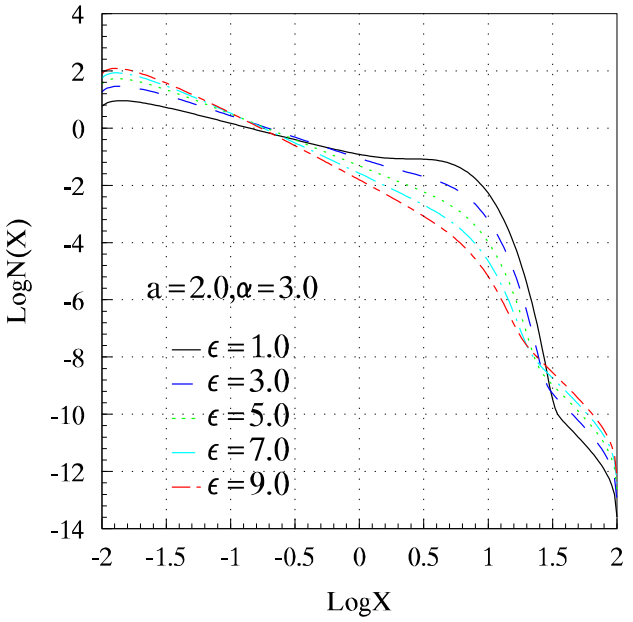

FIG. 1*a*

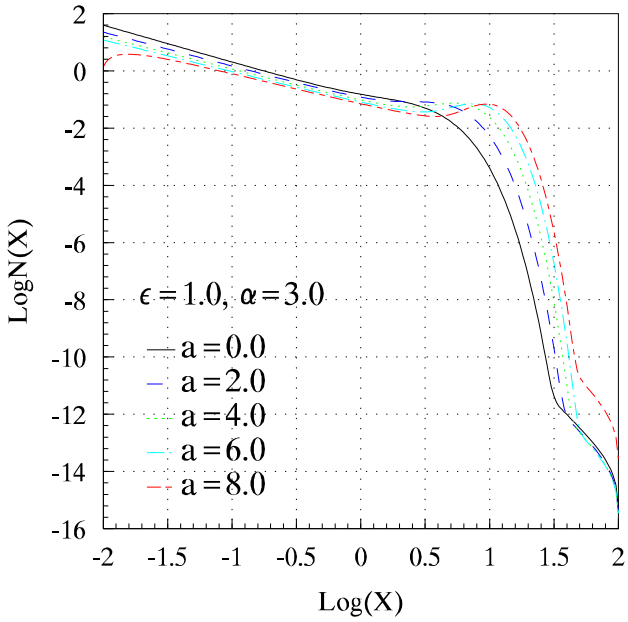

FIG. 1*b*

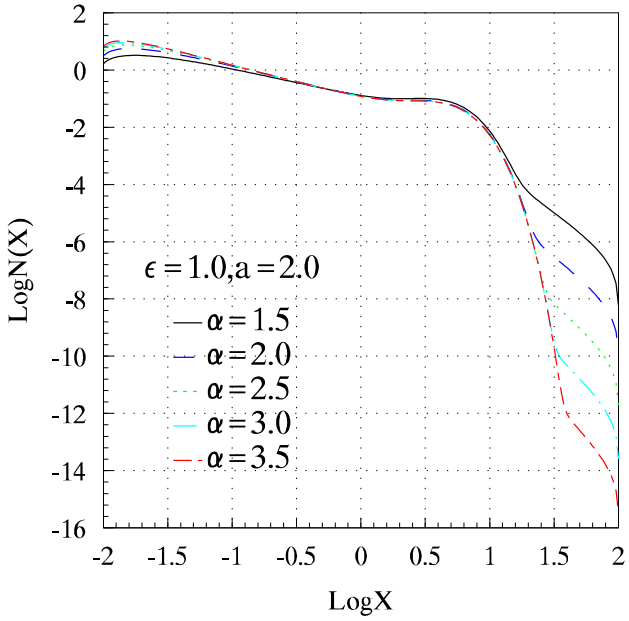

FIG. 1*c*

FIG. 1.—Evolutionary spectra of relativistic electrons. (*a*) Spectra for various values of ε. (*b*) Spectra for various values of a. (*c*) Spectra for various values of the index α. It is assumed that the energy cutoffs of the initial spectrum are $X_1 = 10^{-2}$ and $X_2 = 10^2$.

model was applied to explain abrupt cutoffs of optical-infrared spectra in AGNs (Schlickeiser 1984). The spectra of relativistic electrons for various values of a and ε are shown in Figure 2. It is shown that the momentum at which electron spectrum pileups occur increases with shock wave acceleration a. The peak value increases with ε. It is noticed that the results for the escape time T and the parameter η in § 2.2 are not suitable in case of $\eta < 1$. The basic parameter is ε, which represents the ratio of the acceleration timescale to the electron escape timescale.

3. THE RESULTING SYNCHROTRON SPECTRUM

For a steady state electron density $N(X)$, the synchrotron spectrum is

$$j(Y) \propto \int_{X_1}^{X_2} N(X) F\left(\frac{Y}{X^2}\right) dX \ , \tag{20}$$

where $F(X)$ is the synchrotron radiation spectrum of the single electron with

$$F(X) = X \int_X^{\infty} K_{5/3}(t) dt \ , \tag{21}$$

and Y is the dimensionless frequency defined by $Y = \nu/\nu_c$. The special frequency ν_c is

$$\begin{aligned} \nu_c &= \frac{3}{2}\left(\frac{p_c}{m_e c}\right)^2 \nu_L \sin\theta \\ &= 8.42 \times 10^{10} \eta^{-2} \left(\frac{L}{0.1 \text{ pc}}\right)^{-2} \left(\frac{B}{10^{-3} \text{ G}}\right)^{-1} \\ &\times \left(\frac{n_e}{10^4 \text{ cm}^{-3}}\right)^{-1} \sin\theta \text{ Hz} \ , \end{aligned} \tag{22}$$

where θ is the direction angle of the emission. After the numerical integration for $j(Y)$, we obtain the synchrotron spectra for various values of a and ε that are shown in Figure 3. The spectra have several features: (1) The shape of spectra strongly depends on ε. In the case of short escape lifetimes ($\varepsilon \gg 1$) or weak turbulence, the resulting synchrotron spectrum is weakly affected by the physical processes of the plasma. In the case of long escape lifetimes, which is comparable to the timescale of Fermi acceleration of turbulent plasma ($\varepsilon \sim 1$) or strong turbulence, a flat or weakly inverted spectrum occurs in low frequency ranges determined by a and ν_c. The emissive spectrum in high frequencies is rapidly steepened by the high-energy cutoff of the electron energy spectrum. (2) The range of flat spectrum extends to high frequencies with increasing shock wave acceleration. (3) The spectral shape is weakly dependent on the initial spectral index and energy cutoffs of the relativistic electron distribution.

In terms of our model, the flat-spectrum radio sources have strong plasma turbulence or $\eta \sim 1$. The sources with strong activity and high compactness which may derive strong plasma turbulence tend to be the flat-spectrum radio emission sources. For example, Seyfert galaxies have weaker activity and lower compactness than blazar objects; the flat-spectrum radio sources rarely appear in Seyfert galaxies. But flat-spectrum radio emission is characteristic of blazars.

Extragalactic radio sources are known to vary, at radio wavelength, on timescales ranging from a few days to many years. In general, source variability is associated with size; that is, small sources vary, large sources do not. This has been established by direct VLBI measurements and by well-established relationships between source radio spectrum, size, and variability. Sources with flat or complex radio spectra are small, or have small components, and are variable, while sources with steep spectra are large and less variable (Heeschen et al. 1987). This is consistent with the results of our model: The radio sources with smaller emissive size and magnetic field and lower plasma density tend to produce flat spectra with higher special frequency ν_c.

In blazars, BL Lac objects tend to have a higher percentage of their polarized flux unresolved by VLBI when com-

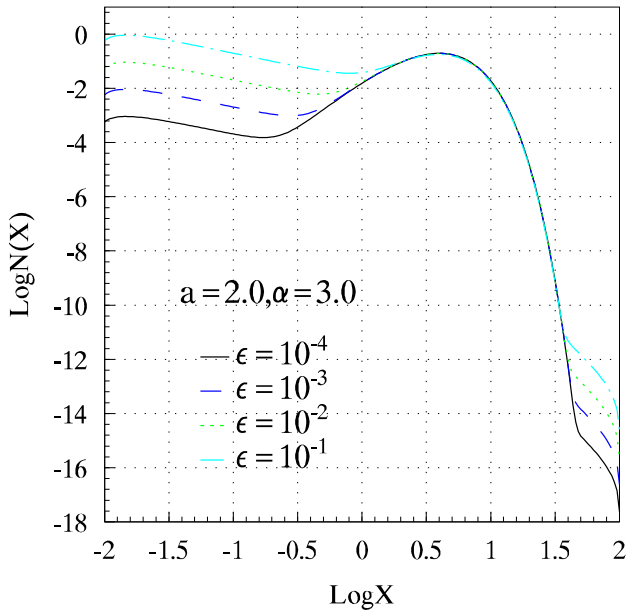

FIG. 2a

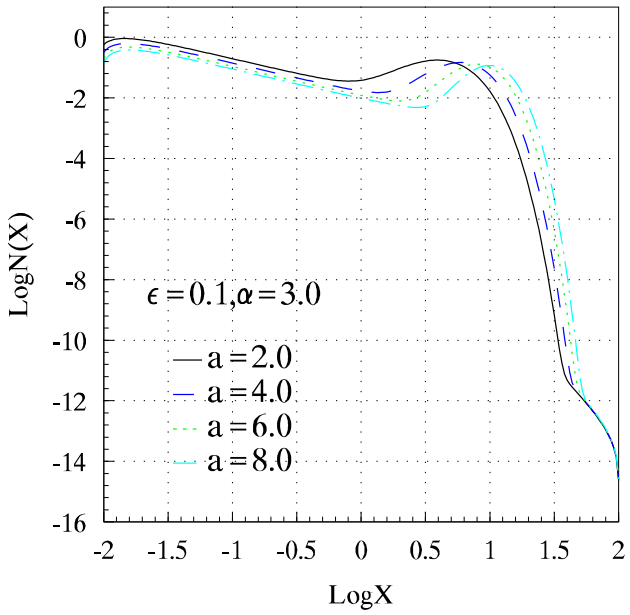

FIG. 2b

FIG. 2.—Evolutionary spectra of relativistic electrons in the case $\eta < 1$; it is assumed that the energy cutoffs of the initial spectrum are $X_1 = 10^{-2}$ and $X_2 = 10^2$. (*a*) Spectra for various values of ε. (*b*) Spectra for various values of a.

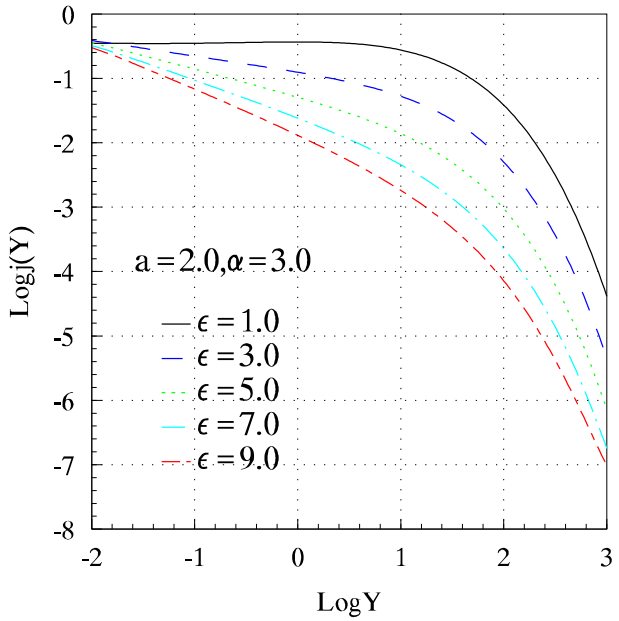

FIG. 3*a*

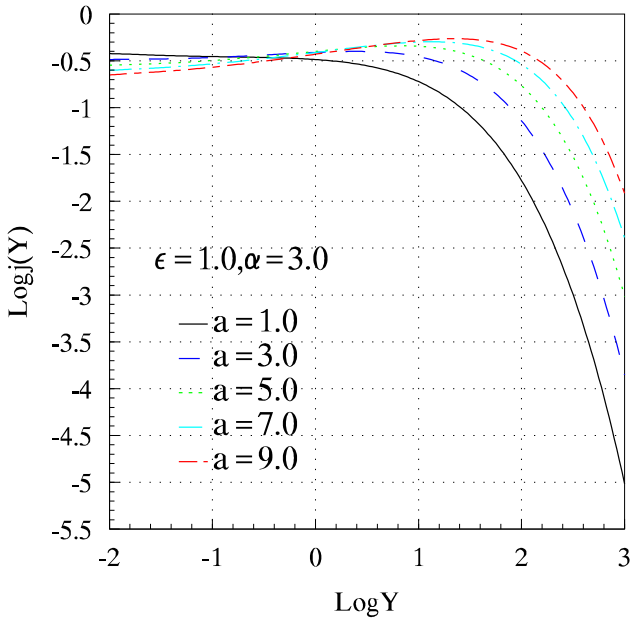

FIG. 3*b*

FIG. 3.—Synchrotron spectra for various values of ε and a. It is assumed that the energy cutoffs of the initial electron spectrum are $X_1 = 10^{-2}$ and $X_2 = 10^2$. (*a*) Spectra for various values of ε. (*b*) Spectra for various values of a.

pared to QSOs (Björnsson 1993; Cawthorne et al. 1993). If their radio emission is related to optically thin synchrotron radiation, radio cores of BL Lac objects should be smaller and have lower plasma density than QSOs; their peak frequency v_c in flat spectra should be higher than those of QSOs statistically. This fact is consistent with the following results: BL Lac objects have flatter spectra between 150 and 375 GHz (Gear et al. 1994), and they are associated with prominent millimeter peaked sources, while QSOs are related to centimeter peak sources (Punsley 1996). We give

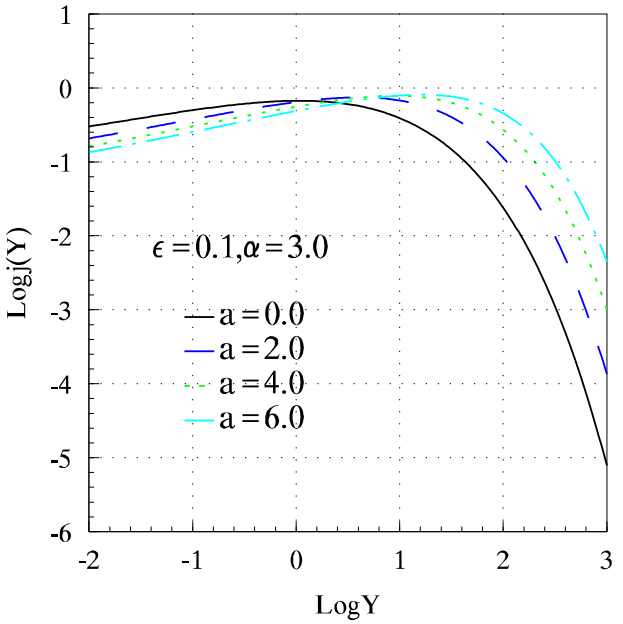

FIG. 4.—Synchrotron spectra for various values of a in the case $\eta < 1$. The assumed parameters are $X_1 = 10^2 - 2$, $X_2 = 10^2$, $\alpha = 3.0$, and $\varepsilon = 0.1$.

their typical parameter values to show the observed difference. Ambient gas in QSOs is the coexistence of dense cool gas ($n_e \simeq 10^8$ cm^{-3}) and hot dilute gas ($n_e \simeq 10^4$ cm^{-3}; Ulrich et al. 1981), while ambient gas in BL Lac objects is cool, diffuse, and highly ionized ($n_e \simeq 10^4$ cm^{-3}; Guilbert, Fabian, & McCray 1983); we take $n_e = 10^5$ cm^{-3} as typical for QSOs, and $n_e = 10^4$ cm^{-3} as typical for BL Lac objects. The large amplitude variability of blazars, at radio wave bands, occurs on timescales ranging from a few days to many years. If this variation is intrinsic to the source, the source size will be small ($L \simeq 10^{-2}$ pc ~ 1 pc) even if the source moves with relativistic speeds; we take $L = 0.1$ pc as typical for them. The estimated magnetic field strength in AGNs is $B \simeq 10^{-3} \sim 10^2$ G, we take $B = 10^{-3}$ G for radio sources of blazars. Therefore we obtain the special frequency $v_c \simeq 100$ GHz for BL Lac objects and $v_c \simeq 10$ GHz for QSOs; the difference in the range of flat spectra is obvious between QSOs and BL Lac objects. Furthermore, it was noted by Punsley (1996) that sources with relatively strong millimeter peaks are tightly correlated with small accretion rates, low nuclear gas densities, high optical polarization, low-luminosity extended radio emission, and a linear polarization along the VLBI jet direction. Because the extended radio sources have lower peak frequency v_c which is beyond wave bands due to their large emissive size, they have steeper radio spectra compared to compact radio sources.

In the Galactic center region, strong plasma turbulence may occur due to the strong activity of nuclei; the radio flat spectrum should be easily formed. In the case $\eta < 1$, the pileup electron spectra produce the inverted synchrotron spectra shown in Figure 4, and its peak frequency is at v_c.

4. CONCLUSION

In this work the mechanisms of radio flat-spectrum sources are examined for the evolution of relativistic elec-

tron spectra in the interplay of second-order Fermi acceleration of turbulent plasma waves, Fermi acceleration of shock waves, radiation losses, particle escape, and adiabatic deceleration in the plasma. We demonstrated that both in blazars and in the Galactic center region, the radio flat spectra are easily formed under the influence of Fermi acceleration of plasma turbulence and shock waves; the timescale of turbulence acceleration is larger than the Alfvén timescale, and the flux of Alfvén waves transfers the maximum power of turbulence into relativistic electrons. The parameter η that shows the level of turbulence determines the spectrum shape of relativistic electron distribution and synchrotron emission.

1. In the case of strong turbulence ($\eta \sim 1$) the flat or weakly inverted spectra are formed in low frequency ranges determined by the typical frequency ν_c and the shock wave acceleration parameter a.

2. In the case of weak turbulence ($\eta \gg 1$) the initial spectra are weakly affected by plasma processes. The flat spectra are not formed.

3. The typical frequency ν_c for the extension of flat spectra is inversely proportional to plasma density, magnetic field, the square of emissive size, and η in the plasma. It determines the difference in radio flat spectral extension between BL Lac objects and high-polarization quasars. The flat spectral extension at millimeter wave bands for BL Lac objects and at centimeter wave bands for high-polarization quasars shows that BL Lac objects have smaller size and lower magnetic field and plasma density.

4. The extended radio sources are necessary to produce steep spectra due to weak turbulence or low typical frequency ν_c that is below self-absorbed frequency or observed frequency.

5. In the case $\eta < 1$, in which the timescale of turbulence acceleration is shorter than the Alfvén timescale, the relativistic electron spectra, as proposed by Schlickeiser (1984), pile up at a momentum at which the timescale for Fermi acceleration and radiation are equal. The inverted spectra of synchrotron emission appear, and its peak frequency is at ν_c.

We wish to thank an anonymous referee for a careful reading of the original manuscript and useful suggestions that enabled us to improve the presentation of this work. The research described in this report was supported in part by the Chinese Science Foundation.

APPENDIX

Kummer's function $M(a, b, z)$ is defined as (Abramowitz & Stegun 1970)

$$M(a, b, z) = \sum_{i=0}^{\infty} \frac{(a)_i}{(b)_i} \frac{z^i}{i!},$$

which is a convergent series for all values of a, b, and z, where $(a)_n = a(a+1)(a+2)\cdots(a+n-1)$, $(a)_0 = 1$.

Define a series A_n:

$$A_n = \frac{(a)_n}{(b)_n} \frac{z^n}{n!},$$

which has a recurrence relation

$$A_{n+1} = A_n \frac{(a+n)}{(b+n)} \frac{z}{n+1}.$$

For a given degree of accuracy ε, if $|A_{N+1}| < \varepsilon$ is satisfied, an approximate value of $M(a, b, z)$ will be

$$M(a, b, z) = \sum_{i=0}^{N} \frac{(a)_i}{(b)_i} \frac{z^i}{i!}.$$

For example, for $z < 10$ and $\varepsilon < 10^{-10}$, $N < 25$ can satisfy the degree of accuracy.

The function $U(a, b, z)$ is defined as

$$U(a, b, z) = \frac{\pi}{\sin \pi b}\left[\frac{M(a, b, z)}{\Gamma(1+a-b)\Gamma(b)} - z^{1-b}\frac{M(1+a-b, 2-b, z)}{\Gamma(a)\Gamma(2-b)}\right]$$

$$= \frac{\Gamma(1-b)}{\Gamma(1+a-b)} M(a, b, z) - \frac{z^{1-b}}{1-b}\frac{\Gamma(b)}{\Gamma(a)} M(1+a-b, 2-b, z),$$

which can be calculated by $M(a, b, z)$.

The integrated function of $M(a, b, z)$ is

$$IM(a, b, \alpha, z) = \int M(a, b, z) z^{\alpha} dz = \frac{z^{\alpha+1}}{\alpha+1} \sum_{n=1}^{\infty} B_n,$$

where

$$B_n = \frac{(a)_n}{(b)_n}\left(\frac{\alpha+1}{n+\alpha+1}\right)\frac{z^n}{n!}$$

is a convergent series for all values of a, b, α, and z. $IM(a, b, \alpha, z)$ is calculated by a method similar to that of calculating $M(a, b, z)$. The integration of $U(a, b, z)$,

$$IU(a, b, \alpha, z) = \int U(a, b, z) z^{\alpha} dz ,$$

is determined by $IM(a, b, \alpha, z)$ using the relation of $M(a, b, z)$ and $U(a, b, z)$.

The distributive function of relativistic electrons is

$$N(X) \propto X^{b-a-2} e^{-X} \left[\int_{X_1}^{X} M(a, b, z) z^{a-\alpha} dz U(a, b, X) + \int_{X}^{X_2} U(a, b, z) z^{a-\alpha} M(a, b, X) \right] .$$

REFERENCES

Abramowitz, M., & Stegun, J. A. 1970, Handbook of Mathematical Functions (Washington, DC: National Bureau of Standards)
Achterberg, A. 1990, A&A, 231, 251
Anantharamaiah, K. R., et al. 1991, MNRAS, 249, 263
Björnsson, C.-I. 1993, ApJ, 416, 104
Cawthorne, T. V., et al. 1993, ApJ, 416, 519
Cotton, W. D., et al. 1980, ApJ, 238, L123
Gear, W. K., et al. 1994, MNRAS, 267, 167
Guilbert, P. W., Fabian, A. C., & McCray, R. 1983, ApJ, 266, 466
Heavens, A. F., & Drury, L. O'C. 1989, MNRAS, 235, 997
Heeschen, D. S., et al. 1987, AJ, 94, 1493
Hughes, P. A., Aller, H. D., & Aller, M. F. 1989a, ApJ, 341, 54
———. 1989b, ApJ, 341, 68
Hughes, P. A., et al. 1991, ApJ, 374, 57
Kellermann, K. I., & Pauliny-Toth, I. I. K. 1969, ApJ, 155, L71
Lesch, H., & Schlickeiser, R. 1985, A&A, 179, 93
Marscher, A. P. 1977, ApJ, 216, 244
Marscher, A. P., & Gear, W. K. 1985, ApJ, 298, 114
Melrose, D. B. 1996, in Extragalactic Radio Sources, ed. R. Ekers et al. (Dordrecht: Kluwer), 423
Melrose, D. B., & Pope, M. H. 1993, Proc. Astron. Soc. Australia , 10, 222
O'Dell, S. L., et al. 1988, ApJ, 326, 668
Punsley, B. 1996, ApJ, 473, 152
Schlickeiser, R. 1984, A&A, 136, 227
Schneider, P. 1993, A&A, 278, 315
Ulrich, M. H. 1981, Space Sci. Rev., 28, 89
Yusef-Zadeh, F. 1989, in IAU Symp. 136, The Center of the Galaxy, ed. M. Morris (Dordrecht: Reidel), 243